A Study in Cloud Phase Parameterization Using the Gamma Distribution

TERRY L. CLARK[1]

Geophysical Fluid Dynamics Program, Princeton University, Princeton, N.J. 08540

(Manuscript received 19 April 1973, in revised form 29 August 1973)

ABSTRACT

A relatively sophisticated cloud phase parameterization scheme based on the gamma distribution is presented which, it is hoped, will eventually make it possible for cloud modellers to include the effects of microphysics more realistically than has been so far possible.

Cloud phase calculations are presented using Lagrangian parcel theory, one-dimensional Eulerian formulation in the vertical, and two-dimensional Eulerian formulation in the horizontal and vertical directions. The solutions obtained using the parameterized scheme were compared with the more conventional finite-difference microphysical calculations of Clark and there was found to be very good agreement for all cases treated.

The efficiency of the scheme allowed a one-dimensional study on the effect of vertical spatial resolution on the prediction of microphysical parameters such as droplet number concentration, mean droplet radius and supersaturation. It was found that poor spatial resolution results in a rather slight underestimation of the droplet number concentration.

1. Introduction

Cloud models which include dynamics as well as microphysical processes, such as those of Árnason and Greenfield (1972) and Clark (1973), require a great deal of calculation even with the present level of precision. If one investigates the present accuracy of these models from the standpoint of calculating nucleation zones as well as regions of droplet evaporation, it is immediately clear that 100 m grid resolution, for example, in the vertical and horizontal is not sufficient but that possibly as much as 10 m resolution is required. This does not mean that the overall results of these models are wrong but only that certain details of the calculations are not well resolved. Also, as far as the resolution of the spectrum of water droplets is concerned, probably a much larger number of categories is required than has been used; otherwise, one cannot ascertain to what degree droplet spectra are correctly calculated by these models. For example, when predicting droplet spectra widths in the first 200 m above cloud base, one would like to be sure that the spectra widths were determined by the assumed physical equations and not by numerical dispersion. It is important to note that poor spatial resolution has a strong effect upon the droplet radius domain calculations when we consider that the characteristic time for water particles to pass through a given radius domain range can be much smaller than the time required to pass through a single grid point. This effect would be particularly strong in regions of nucleation and droplet evaporation where rapid droplet growth or evaporation can cause droplets to pass through many Eulerian radius categories in the space of 100 m. This argument suggests that increased resolution in the spectral domain should be accompanied by increased resolution in the spatial domain so that the substantial time derivative of each particle category is more accurately represented. This approach is only possible with one-dimensional models where computation time and storage requirements are not too severe. (See the Appendix for a more detailed discussion of truncation errors associated with microphysical finite-difference Eulerian cloud models.) This rather brief criticism of two-dimensional, finite-difference, microphysical-dynamical cloud models suggests the need for a more practical method of treating the cloud phase processes which for low spatial resolution will give essentially equivalent results. The need for a more practical scheme for treating the microphysics is even more obvious when one considers extending these models into three spatial dimensions where hopefully one will be able to compare calculations more readily with nature. It was this latter point which was the main incentive for the development of the parameterization scheme presented in this paper.

Kessler (1967) proposed a parameterization scheme where the cloud phase is represented by the single parameter q_c, the mixing ratio of cloud water to air. Autoconversion from cloud water to rain water was treated empirically by assuming a conversion rate dependent on the value of q_c. Berry (1965) and Cotton (1972) have suggested more sophisticated auto-

[1] Present affiliation: Atmospheric Environment Service, Downsview, Ontario, Canada.

conversion rates which empirically include the effects of droplet number concentration and cloud-droplet radius dispersion. It is the author's contention that in order to significantly improve the warm rain parameterization schemes such as those of the above authors, a more physically representative cloud phase scheme is needed where the cloud droplet number concentration and radius dispersion are model-predicted from the initial cloud condensation nuclei (CCN) distributions.

The present paper presents a cloud phase parameterization based on the gamma distribution which represents the cloud droplet distributions. The supersaturation of the air with respect to a plain water surface is considered which allows a prediction of the droplet concentrations produced through nucleation of the assumed CCN. The coefficients of the gamma distribution are considered as field variables which allows prediction of the droplet distribution mean radius and to a lesser extent the radius dispersion. In addition, it is possible that this scheme is as accurate (or could be made so) as the pure finite-difference method of treating the droplet distribution because some of the problems associated with radius domain resolution are either lessened or altogether eliminated. For example, in a poorly resolved nucleation region it seems conceivable that better results could be obtained by using an assumed type of droplet distribution than by the usual finite-difference approaches of Árnason and Greenfield (1972) or Clark (1973). In the distribution approach one is treating integrated variables (such as droplet number concentration and mean radius, etc.) which have longer time scales than integrated number concentrations over say a 1-μm radius interval.

Since it is not possible at present to evaluate the representativeness of a model by direct comparison with nature, the author chose to assess the parameterized scheme by comparison of solutions with more conventional finite-difference microphysical solutions. For this purpose the Clark (1973) microphysical model will be used as a qualitative gauge of the representativeness of the parameterized solutions.

The gain in computational speed (crudely estimated as 10 times faster than the Clark nucleation, condensation and evaporation calculations) and the gain in computer storage (4 field arrays instead of the approximately 65 used for nuclei and droplets in the Clark model) allowed a study on the effect of using low spatial resolution in microphysical cloud models such as those of Árnason and Greenfield (1972) and Clark (1973). This is considered an important problem in the field of cloud modelling because using the current numerical techniques it appears to be quite impractical to resolve the small spatial dimensions likely to exist in nucleation zones as well as evaporation regions. Thus, it is important to understand the effects of using such poor resolution as, say, 100 m grids on the prediction of microphysical parameters before one can thoroughly evaluate the results of such microphysical models. The results of this paper are considered encouraging to the continued microphysical modelling of clouds.

2. Parcel theory application of cloud phase parameterization

The main assumption in formulating the cloud phase parameterization is that the spectra of droplets can be described by the gamma distribution for all time and space. The gamma distribution has three variable parameters which allows time dependency (and space dependency for the Eulerian case) for the number concentration N of the droplets, their mean radius $\bar{R}$, and the spectrum width which is described by the coefficient of dispersion μ which is given as

$$\mu=(\overline{R^2}/\bar{R}^2-1)^{\frac{1}{2}}. \tag{1}$$

All other characteristics of the droplet spectrum can be described in terms of these three parameters. The distribution function is given as

$$f\langle r\rangle=\frac{N\beta^{\alpha}r^{\alpha-1}}{\Gamma(\alpha)}\exp(-\beta r), \tag{2}$$

where $f\langle r\rangle dr$ is the number of droplets cm^{-3} between radii r and $r+dr$, Γ is the gamma function, and N the total number of droplets cm^{-3} between $r=0$ to $r=\infty$. The pth moment of the distribution is given by

$$\overline{R^p}=\frac{\Gamma(\alpha+p)}{\Gamma(\alpha)\beta^p}, \tag{3}$$

and

$$\mu^2=1/\alpha. \tag{4}$$

Levin (1958) has observed that the gamma distribution gives a rather good fit to *observed* droplet spectra with α ranging between 6 to 10. The procedure in this section will be to let α range anywhere from 3 to 400 even though values larger than 10 may not be found in nature. The reason for letting α have such a wide range is to show how accurately the parameterized solutions for N, $\bar{R}$, μ, q_c and S compare with the solutions of a high-radius-resolution, finite-difference model. The problem of spectrum broadening of cloud droplets is still one of the main unsolved problems of cloud physics and will not be attempted in this paper. Thus, it is the intent of this paper to solve the *specified* governing equations (which do not predict broad spectra) as accurately as possible in the framework of this parameterization.

The equations governing the droplet distribution moments are derived from the kinetic equation (velocity divergence assumed zero in this section)

$$\frac{df}{dt}\langle r\rangle+\frac{\partial}{\partial r}\left(f\langle r\rangle\frac{dr}{dt}\right)=0, \tag{5}$$

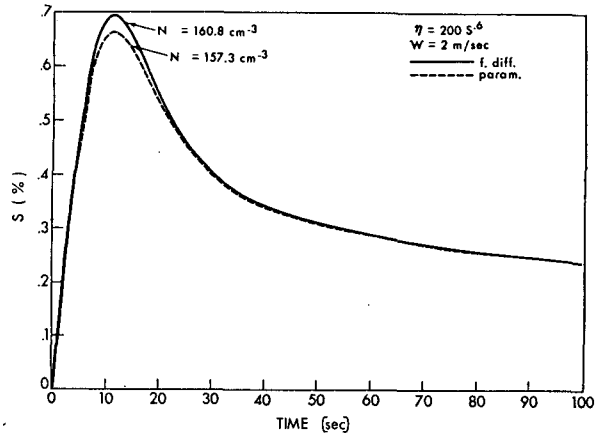

FIG. 1. Lagrangian parcel solutions of S vs t for a constant vertical velocity of 2 m sec^{-1} and a maritime CCN distribution.

where

$$\frac{dr}{dt}=\frac{k}{r}\left(S-\frac{a}{r}\right), \tag{6}$$

where $k=0.98$ (μm)^2 sec^{-1}, $a=0.115$ μm, and S is the percent supersaturation. The equations governing the first two moments of the droplet distribution are found from (5) and (6) to be

$$\frac{d\bar{R}}{dt}=k(S\overline{R^{-1}}-a\overline{R^{-2}})-\bar{R}\frac{d\ln N}{dt}, \tag{7}$$

$$\frac{d}{dt}\overline{R^2}=2k(S-a\overline{R^{-1}})-\overline{R^2}\frac{d\ln N}{dt}. \tag{8}$$

Combination of (3), (7) and (8) result in

$$\frac{d\beta}{dt}=\frac{3kS\beta^3}{\alpha(\alpha-1)}-\frac{5ka\beta^4}{\alpha(\alpha-1)(\alpha-2)}-\alpha\beta\frac{d\ln N}{dt}, \tag{9}$$

$$\frac{d\alpha}{dt}=\frac{4kS\beta^2}{(\alpha-1)}-\frac{6ka\beta^3}{(\alpha-1)(\alpha-2)}-\alpha(\alpha+1)\frac{d\ln N}{dt}. \tag{10}$$

Nucleation is treated by letting

$$\frac{dN}{dt}=-\frac{d\eta}{dt}, \tag{11}$$

where η is the cumulative number of condensation nuclei available for nucleation below the supersaturation S, and is a function of time in the sense that once a certain number of nuclei have been activated, then these nuclei are no longer available for future nucleation unless a nuclei source is considered. In later sections of this paper, the spatial dependence of η will include the fact that the critical supersaturation S_c for a given salt mass (NaCl assumed) is a function of the temperature; for non-Lagrangian calculations advection is also considered.

In practice, the method of treating η is to let it equal the total number of nuclei available for nucleation over a wide range of supersaturation. In order to decide how many nuclei are actually available for nucleation below a given S value a table is used which contains the information on how large η should be for different S values. In computing, this method involves one field array η plus one table and is easiest to apply when homogeneous initial conditions are assumed for the nuclei. In the present section no temperature dependence for S_c has been considered.

Two cases for initial cumulative number distributions η are treated; for the first η is given by

$$\eta=200S^{0.6}, \tag{12}$$

taken from Warner (1969), representing maritime conditions, and for the other

$$\eta=2000S^{0.4}, \tag{13}$$

from Twomey (1959), representing continental conditions. These distribution functions are good approximations to observational data only above a finite value of S_c and do not necessarily apply to large and giant salt nuclei. In the present parameterization, no account will be taken of salt mass in the droplet growth equation, so (12) and (13) will be used from $S_c=0$ up to whatever maximum value of S_c that might occur in the calculations. This approximation might be considered equivalent to assuming there are very few large CCN. To be consistent the same physical assumptions will be applied to the more conventional Lagrangian model which is used as a gauge of the accuracy of the parameterization scheme. As will be seen, due to the exclusion of large and giant salt particles, the conventional Lagrangian model required rather high radius resolution in order to resolve the very narrow resulting spectra.

To complete the system of equations for the Lagrangian model, in which parcel ascent is considered,

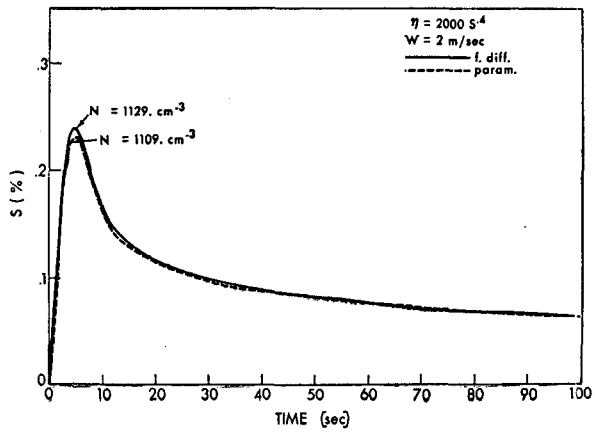

FIG. 2. As in Fig. 1 except for a continental CCN distribution.

we have the equation for S (see, e.g., Fletcher, 1962),

$$\frac{dS}{dt}=T_S-H_2C_d, \tag{14}$$

where

$$\left.\begin{aligned} T_S&=H_1w, \qquad H_2=2.69\times10^4 \\ H_1&=0.05\%\ \text{m}^{-1}, \quad w=2\ \text{m sec}^{-1} \end{aligned}\right\} \tag{15}$$

were assumed. C_d is the condensation-evaporation rate and is given by

$$C_d=\frac{dq_c}{dt}, \tag{16}$$

where q_c is the cloud water mixing ratio. In terms of the gamma distribution

$$\begin{aligned} q_c&=\frac{4}{3}\frac{\pi10^{-12}}{\rho}\frac{(\alpha+1)(\alpha+2)}{\alpha^2}N\bar{R}^3, \\ &=\frac{4}{3}\frac{\pi10^{-12}}{\rho}N\overline{R^3}, \end{aligned} \tag{17}$$

where ρ is the ambient air density, and N is in cm^{-3} and $\bar{R}$ in μm.

In this parameterization formulation, the first and second moments of the distribution are calculated explicitly through (9) and (10), whereas the derived third moment of the distribution q_c is used for C_d adjustments of water vapor, liquid water and temperature. Inaccuracies in determining q_c are eliminated through (14) because of the strong negative feedback effect of the supersaturation field. Thus, this method results in accurately predicting the four variables N, $\bar{R}$, $\overline{R^2}$, $\overline{R^3}$ within the constraining assumption that the gamma distribution is obeyed.

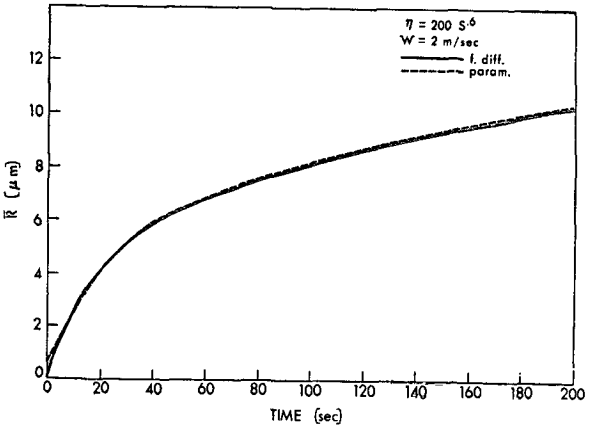

FIG. 3. Lagrangian parcel solution for $\bar{R}$ vs t for a maritime CCN distribution.

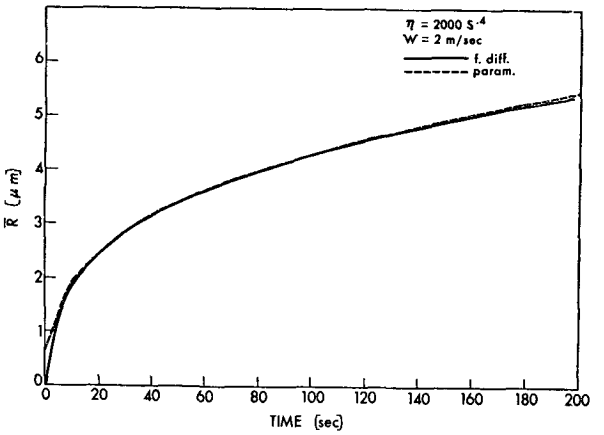

FIG. 4. As in Fig. 3 except for a continental CCN distribution.

Initial conditions have to be specified before a solution can be obtained using this scheme. The following initial conditions were arbitrarily chosen as

$$N=1\ \text{cm}^{-3}, \quad \bar{R}=0.6\ \mu\text{m}, \quad \alpha=3. \tag{18}$$

The scheme was tested against a finite-difference model where 1000 radius increments of $\Delta r=0.05\ \mu$m each were considered. The formulation of this model is straightforward and will not be described in detail in this paper. A similar numerical formulation used by Clark (1973) was applied except that instead of the logarithmic radius increments used by Clark, equal radius increments of 0.05 μm from $r=0.6$ to 50 μm were employed in this section. Since the effects of salt mass on the diffusional growth of droplets is ignored, it was assumed that transfer occurs from the cumulative number distribution of CCN to the smallest radius value in the droplet domain.

Figs. 1 and 2 show a comparison between the parameterized solutions and the finite-difference solutions of S for the maritime and continental cases, respectively. There is surprisingly good agreement between the solutions, with the main difference being that the parameterized solutions predicted the maximum values of S to be $\sim5\%$ smaller than the finite-difference values. The reason for this slight difference is probably due to the choice of initial conditions (18). The values for N which were reached (and maintained constant) after $S_{\max}$ was passed are shown in the figures for each case.

Figs. 3 and 4 show the comparisons for $\bar{R}$, where once again there is very good agreement. The comparisons for q_c are not shown but were found to be the most accurately predicted variable by this parameterization scheme.

Fig. 5 compares the parameterized and finite-difference solutions for μ. Here we see by far the largest difference, although in the author's opinion there is still very good agreement considering two points. First, we are comparing against an extremely highly resolved

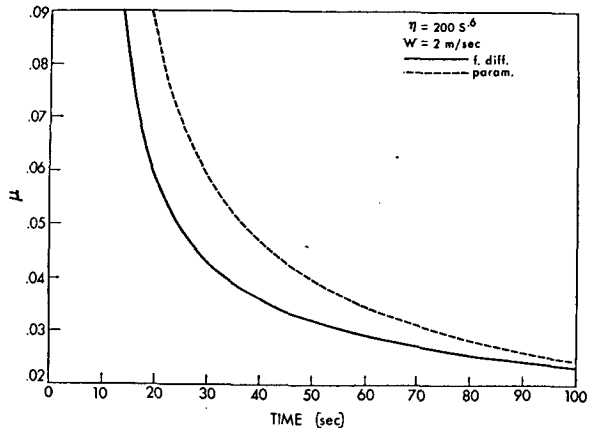

FIG. 5. Lagrangian parcel solutions for μ vs t for a maritime CCN distribution.

finite-difference scheme. For example, it was found that if 0.5 μm radius grids were used for the finite-difference scheme then μ leveled off at approximately 0.05. Thus, it is important to remember that the conventional finite-difference schemes require very high resolution before one can realistically talk about predicting μ according to the specified governing equations. If one uses low resolution, in the radius domain, then the truncation error essentially determines μ. Second, there is a problem of specification of initial conditions for α. If the initial minimal value of $\alpha=3$ was increased to a somewhat higher value, say 4, then the two curves would be in much better agreement. The reasoning behind this point is that once nucleation is completed [neglecting the curvature effect in (9) and (10)] then it can be shown that μ is inversely proportional to $\bar{R}^2$. Therefore, increasing the initial value of α will have the effect of shifting the parameterization solution of μ closer to the finite-difference solution. The indications are that this proposed parameterization scheme solves Eqs. (5) and (6) very accurately when compared to a highly resolved finite-difference scheme (say $\Delta r=0.05$ μm) under the specified physical assumptions.

The next sections will consider the extension of this parameterization to an Eulerian formulation in which the Lagrangian time derivative is replaced by a local time derivative plus an advection term. The effect of vertical resolution will then be studied in order to ascertain the qualitative effect of using low spatial resolution in a multi-spatial dimensioned, microphysical cloud model when the nucleation region is poorly resolved.

3. Eulerian formulation of the parameterized model in a kinematical framework

The governing equations for the spectrum parameters are derived from the kinetic equation

$$\frac{\partial f}{\partial t}+\nabla\cdot(\mathbf{V}f)+\frac{\partial}{\partial r}\left(f\frac{dr}{dt}\right)=\nabla\cdot(K\nabla f), \tag{19}$$

which has been generalized from (5) to include divergent flow as well as an eddy mixing term. $\mathbf{V}$ is the wind velocity and K the eddy mixing coefficient which will be assumed constant in this paper. The diffusional growth rate for the droplets is given by

$$\frac{dr}{dt}=\frac{k}{r}\left(S-\frac{a}{r}\right), \tag{20}$$

where S is the supersaturation, and k and a are functions of environmental pressure and temperature. For comparison purposes, the identical functional form is used for k and a as used by Clark (1973).

Multiplying (19) by 1, r and r^3, and integrating from $r=0$ to ∞, we obtain

$$\frac{\partial N}{\partial t}+\nabla\cdot(\mathbf{V}N)=C_\eta+\nabla\cdot(K\nabla\cdot N), \tag{21}$$

$$\frac{\partial(N\bar{R})}{\partial t}+\nabla\cdot(\mathbf{V}N\bar{R})=Nk(S\overline{R^{-1}}-a\overline{R^{-2}})+\nabla\cdot(KN\bar{R}), \tag{22}$$

$$\frac{\partial}{\partial t}(\rho q_c)+\nabla\cdot(\rho\mathbf{V}q_c)=\rho C_d+\nabla\cdot(K\nabla\rho q_c), \tag{23}$$

where (21) represents the conservation of droplet numbers, (22) the equation for $N\bar{R}$, and (23) the conservation of cloud water. C_η represents the nuclei source-sink term which depends on the supersaturation for the production of droplets during condensation. During evaporation, all droplets are assumed to go back into nuclei once enough evaporation has occurred to reduce q_c to the initial value assumed in (18). A similar equation to (21) is assumed for the cumulative number distribution of condensation nuclei η, such that

$$\frac{\partial\eta}{\partial t}+\nabla\cdot(\mathbf{V}\eta)=-C_\eta+\nabla\cdot(K\nabla\eta). \tag{24}$$

Eqs. (21) plus (24) guarantee exact conservation of the total number of nuclei plus droplets in a closed domain.

It is more appropriate to advect $\bar{R}$ instead of $N\bar{R}$ in a numerical model because $\bar{R}$ is less susceptible to spatial truncation error than $N\bar{R}$. The reason for this is the spatial gradients of $\bar{R}$ are very much smaller in magnitude than those of $N\bar{R}$. In continental clouds the ratio of these gradients could be as much as three orders of magnitude. Combining (21) and (22), we arrive at

$$\frac{\partial\bar{R}}{\partial t}+\nabla\cdot(\mathbf{V}\bar{R})=\bar{R}\nabla\cdot\mathbf{V}+k(S\overline{R^{-1}}-a\overline{R^{-2}})-\frac{R}{N}C_\eta+\frac{1}{N}\nabla\cdot(K\nabla N\bar{R})-\frac{\bar{R}}{N}\nabla\cdot(K\nabla N). \tag{25}$$

A prediction equation for $\overline{R^2}$ is not used because once N, $\bar{R}$ and q_c are defined at a point, $\overline{R^2}$ is derived

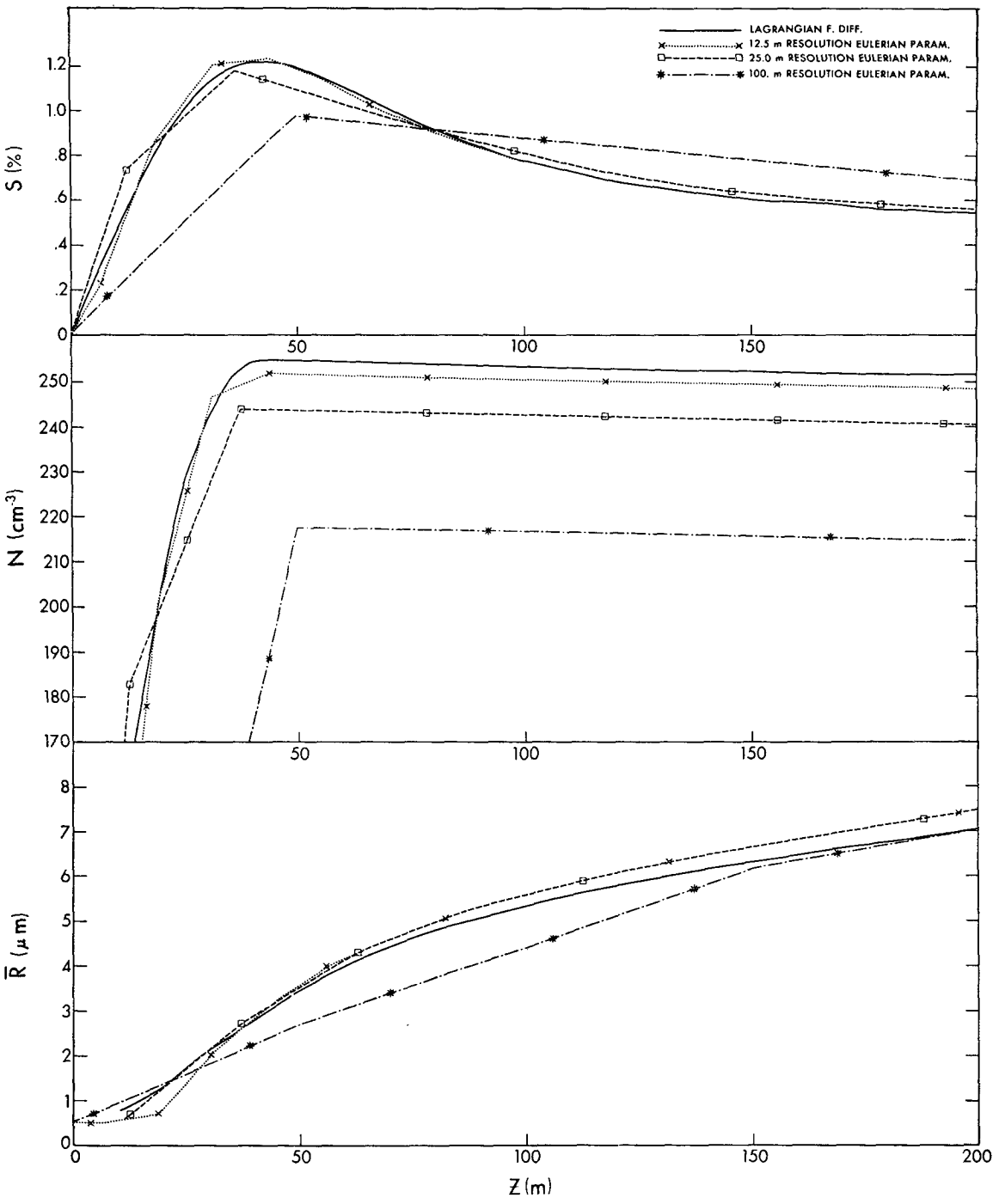

FIG. 6. Solutions of S, N and $\bar{R}$ in a one-dimensional vertical column where the vertical mass flux of air is constant. Solutions for steady state are shown for 100, 25 and 12.5 m vertical resolution using the parameterized model. The equivalent finite-difference (radius domain) Lagrangian (in time) solutions are shown as solid lines.

through the gamma distribution. Actually, $\overline{R^2}$ is never explicitly used in the calculations. It was found more convenient to use N, $\bar{R}$, q_c, α and β.

As in the Clark (1973) model, the T_S prediction is taken from the equations for potential temperature and mixing ratio of water vapor. These equations are given as

$$\frac{\partial\theta^*}{\partial t}+\frac{\nabla\cdot(\rho\mathbf{V}\theta^*)}{\rho}=\frac{LC_d}{C_p\bar{T}}+\frac{\nabla\cdot(\rho K\nabla\theta^*)}{\rho}, \tag{26}$$

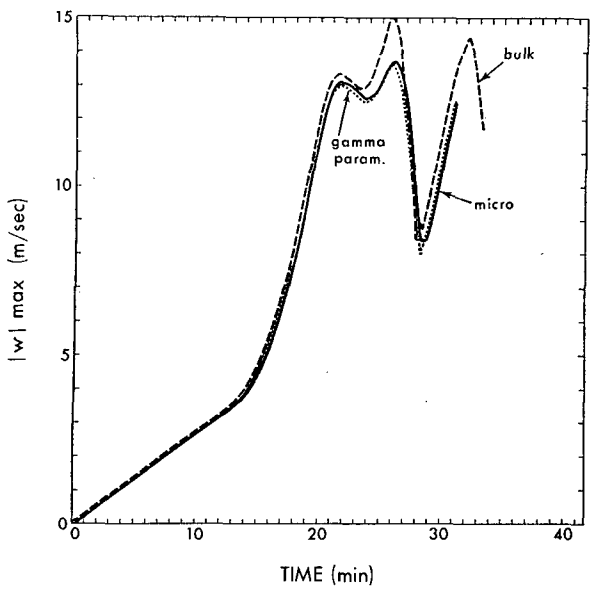

FIG. 7. Maximum vertical velocity $|w|_{\max}$ vs t for runs I and II from Clark (1973), and the present two-dimensional parameterized solution.

$$\frac{\partial q_v}{\partial t}+\frac{\nabla\cdot(\rho\mathbf{V}q_v)}{\rho}=-C_d+\frac{\nabla\cdot(\rho K\nabla q_v)}{\rho}. \tag{27}$$

The saturation mixing ratio of water vapor, q_{v_s}, was taken as

$$q_{v_s}=q_{v_0}(z)\exp[(L/R_v\bar{T})\theta^*], \tag{28}$$

and the supersaturation as

$$S=[(q_v/q_{v_s})-1)], \tag{29}$$

where θ^* is the ratio of the perturbation potential temperature and the layer mean value Θ, and $\bar{T}$ the environmental temperature.

The parameterization scheme will now be summarized. First, we initialize N, $\bar{R}$, q_c, η, θ^* and q_v. The next step is to advect and diffuse N, q_c, η, $\bar{R}$, θ^* and q_v through Eqs. (21), and (23) to (27), respectively. The next step is to calculate a dynamic supersaturation tendency T_S which is to be used for condensation-evaporation and nucleation calculations. The parameters α and β of the gamma distribution are also calculated using the new values of N, $\bar{R}$ and q_c. Through Eqs. (9), (10), (11) and (14), the new values of $\bar{R}$, N, η and q_c are calculated. The final step is to adjust θ^* and q_v using C_d in (26) and (27), respectively. The finite-difference methods used by Clark (1973) were used for the treatment of the equations. This involves centered time and space derivatives for θ^* and q_v, and second-order Crowley (1968) advection with forward time steps for N, $\bar{R}$, η and q_c. The dynamic tendency term T_S for the supersaturation equation was determined as the difference between the future S due to advection, adiabatic cooling and diffusion and the advected past S divided by the large dynamic time step. Small forward time steps were used for the explicit treatment of the condensation-evaporation and nucleation calculations. H_2 was derived according to Clark (1973) so that we are insured the large time step S values and the short time step S values are consistent at the proper time levels. For further details about the numerical scheme we refer the reader to Clark.

Some of the weaknesses and problems associated with the proposed scheme will now be outlined.

1) As already mentioned, one of the problems still troubling cloud physicists is how nature develops such broad droplet spectra in the initial phases of convection. The equations outlined in this paper do not appear to account for broad spectra and this leads to a technical problem when treating the equations numerically. Truncation error due to advection can produce unrealizable spectra widths, i.e.,

$$\tfrac{4}{3}\pi 10^{-12}N\bar{R}^3>\rho q_c; \tag{30}$$

if we compare (17) and (30), values of $\alpha<0$ can result. An adjustment scheme was implemented after each advection calculation so that the minimum allowable coefficient of dispersion μ was arbitrarily set equal to 0.05. This adjustment was carried out by decreasing $\bar{R}$ (and when necessary also decreasing N) so that the predicted value μ was always greater than 0.05 after advection. Once the physics for droplet spectrum broadening is well understood, it is hoped that the physics can be included in the parameterization so that the above-mentioned weakness will be considerably reduced.

2) During nucleation, spectral broadening can occur to the point where α becomes too small. Since Eqs. (9) and (10) become indeterminate at $\alpha=2$, nucleation was not allowed to broaden the spectrum beyond the arbitrary value of $\alpha=3$. Once salt mass effects are included in the gamma parameterization, this problem will most likely be resolved.

3) Spatial truncation error can and does lead to meaningless predictions for N, η, $\bar{R}$ and q_c unless one chooses to use highly diffusive differencing schemes such as upstream differencing. Negative values for N, η, $\bar{R}$ and q_c occur notably near cloud boundaries where the gradients of these variables are very large. A conservative hole filling scheme, as employed by Clark (1973), was used to correct for these deficiencies. The author doubts that two- and, especially, three-dimensional cloud models will be able to adequately resolve the gradients in N, η and q_c near cloud boundaries for decades to come. Five to ten meter spatial grid resolution would probably be necessary to accurately model the strong gradients mentioned. This is completely impractical on even the most advanced computers of the day when considering the modelling of even a relatively small cumulus cloud. Thus, the above-mentioned weakness is not a weakness particular to this cloud model but

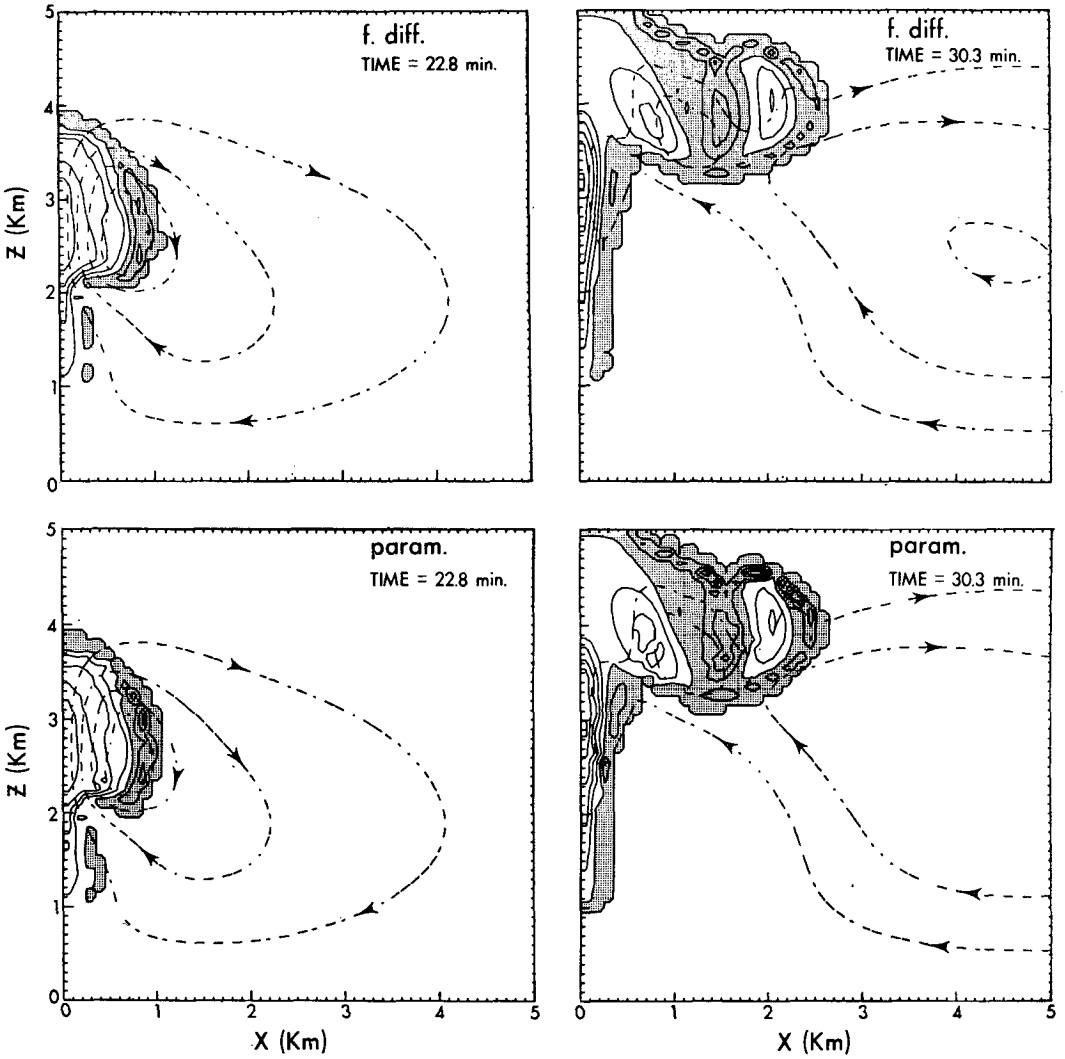

FIG. 8. Comparison of condensation-evaporation rates for run II of Clark (1973) and the present two-dimensional parameterized solution. Contour interval is 5×10^{-6} sec^{-1}. Negative regions are shown by shading.

a weakness of all present day microphysical cloud models (for two or three spatial dimensions) and we must learn to deal with the problem.

4) One of the main weaknesses of the parameterization is that a single gamma distribution was assumed. This led to the explicit treatment of N, $\bar{R}$ and q_c during advection whereas during condensation-evaporation the explicit treatment of N, $\bar{R}$ and $\overline{R^2}$ was considered. As previously mentioned, q_c is accurately treated during condensation-evaporation because of the strong negative feedback effect of S. Therefore, during advection and diffusion we are heavily relying on the assumption of the gamma distribution holding, from which we derive the prediction of $\overline{R^2}$. Mathematically, such a scheme can probably not be justified, but on the other hand, as will be seen, the qualitative as well as quantitative results obtained by using the scheme appear to be at least as acceptable as those obtained for the explicit treatment of 20–40 *droplet* category number concentrations where truncation error in the radius domain can be rather large. This deficiency could possibly be corrected by considering more than one gamma distribution so that the number of degrees of freedom is increased. Of course, the author recognizes that the real advantage of using a large number of droplet category number concentrations lies in the fact that this type of model has a much better chance of simulating nature as the model's resolution is increased.

4. Effect of spatial resolution and convergence of the solution for a one-dimensional kinematical model

A one-dimensional vertical column is considered where the half-width of the column is kept constant at 100 m. The vertical height considered is 5 km with

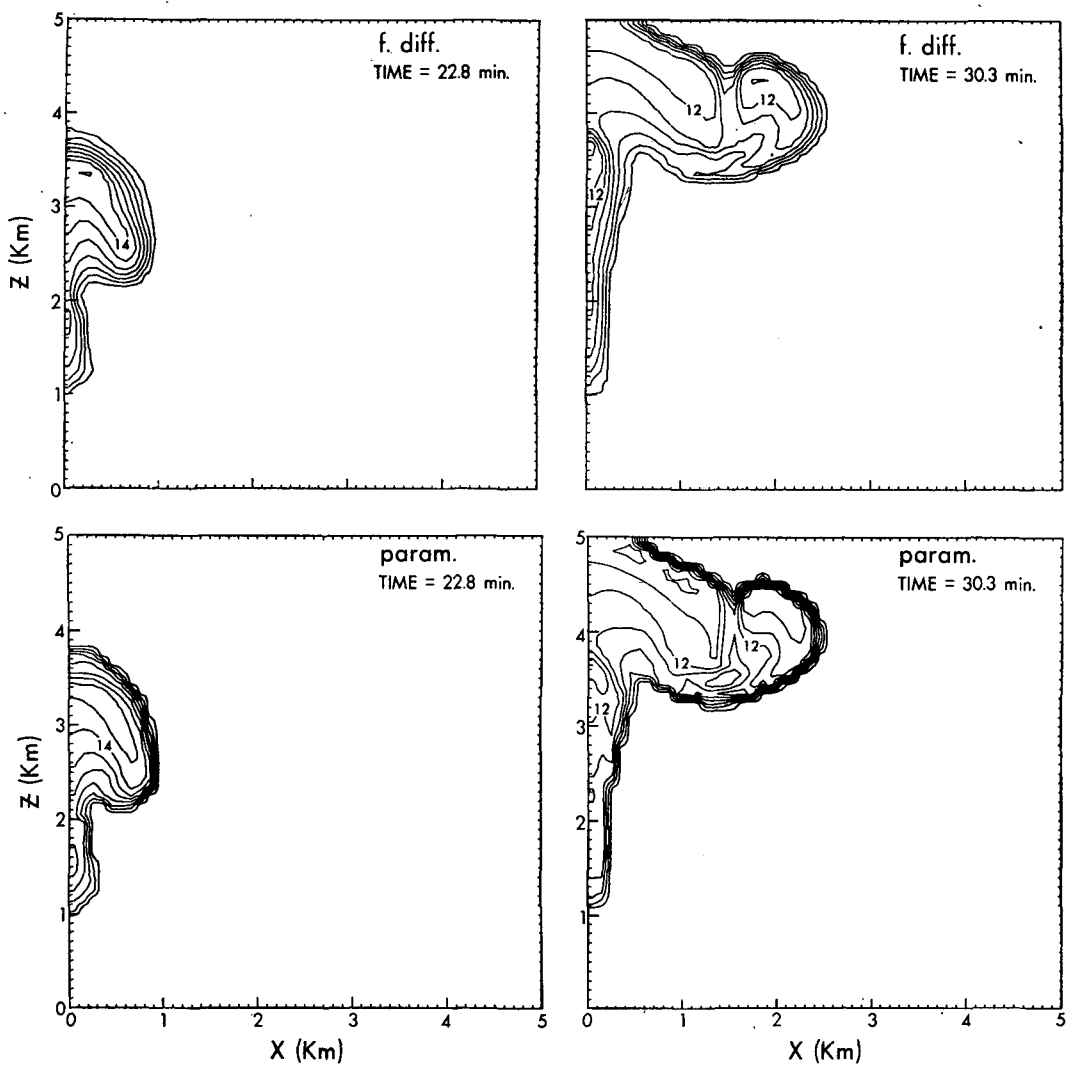

FIG. 9. As in Fig. 8 except for $\bar{R}$ fields with a contour interval of 2 μm.

inflow occurring into the column from the sides in the first 100 m of height and outflow occurring from the sides in the last 100 m. The mass flux in the column was kept constant with height by letting

$$\rho w = 5 \times 10^{-3} \text{ m gm cm}^{-3} \text{ sec}^{-1}. \quad (31)$$

The initial conditions for θ^* and q_v were taken as identical to those used by Clark. This gives the first 1 km of height as a neutrally stable layer with the relative humidity ranging from 68% at the ground to 87% at the 1-km level. The next 3 km was taken as a conditionally unstable layer to moist convection with a constant potential temperature lapse rate of 3.3C km^{-1}. The relative humidity ranged linearily from 87% at the 1-km level to 80% at the 2-km level, after which it remained constant at 80% up to the 4-km level. From 4 to 5 km the layer was assumed isothermal with the relative humidity varying from 80% to 40%. The initial nuclei distribution was adapted from Warner (1969) and was represented by

$$\eta = 200(\bar{T}/273)^{1.5} S^{0.6}. \quad (32)$$

The assumed temperature dependence in (32) was chosen primarily because it gave a reasonably good fit to the vertical variation of η used by Clark (1973). The initial conditions as specified by (18) were used for N, $\bar{R}$ and α.

This numerical framework will be used to study the steady-state solutions for N, $\bar{R}$ and S which will then be compared with an equivalent Lagrangian finite-difference model for the first 200 m above cloud base. Cloud base was approximately at the 825 m level. From this comparison we can deduce some of the qualitative effects of low spatial resolution on the predictions of the microphysical parameters. Three Eulerian type calculations were performed with 100, 25 and 12.5 m vertical grids using the parameterized cloud phase model. Also considered is a finite-difference Lagrangian model

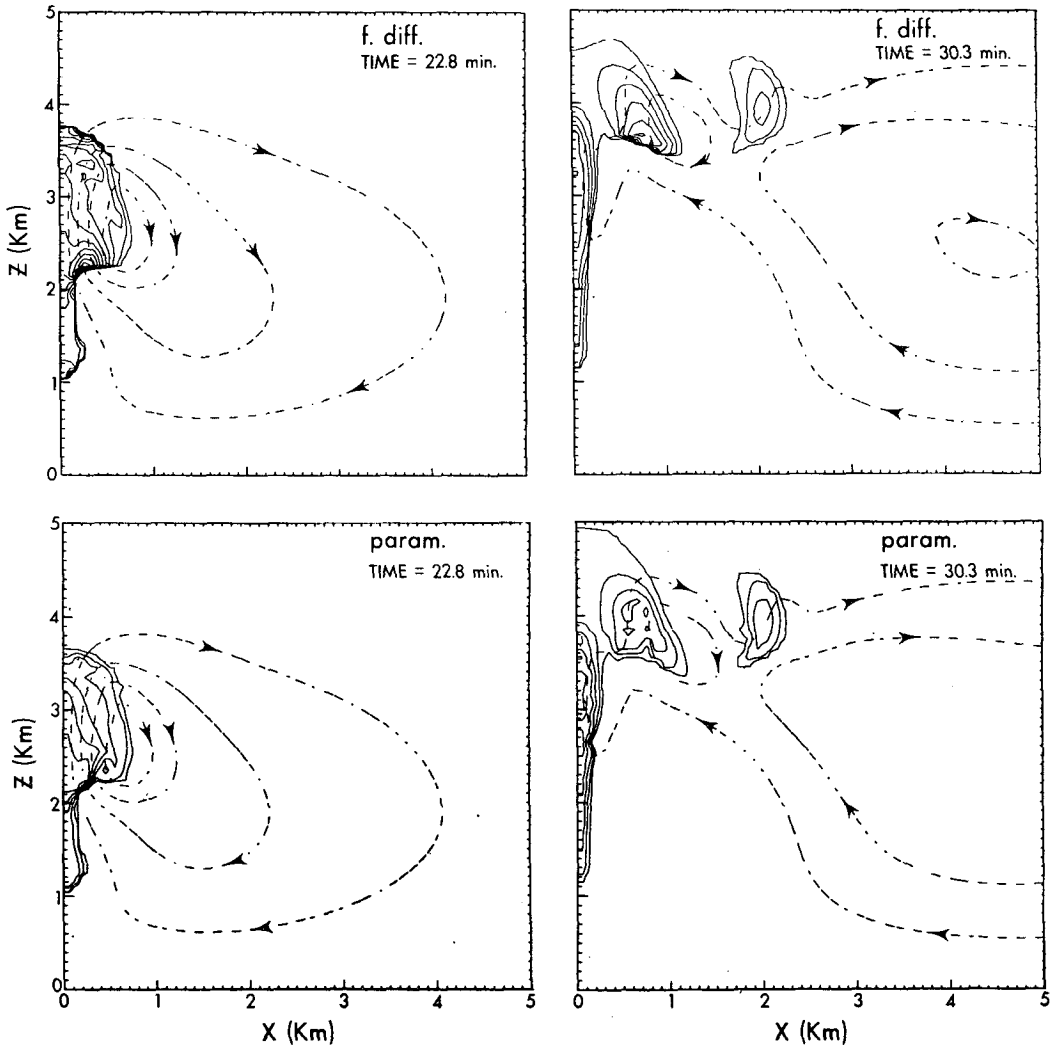

FIG. 10. As in Fig. 8 except for S fields with a contour interval of 0.2%.

where 100 droplet categories were considered with 0.5 μm radius grid resolution assumed. The reason for the choice of 0.5 μm radius increments was to make the finite-difference minimum values of μ approximately correspond to the arbitrary cutoff value of $\mu=0.05$ used for the parameterized model. Adiabatic expansion, changes with height above cloud base of vertical velocity, as well as the thermodynamic variables, were made to correspond as closely as possible to the Eulerian model. The main difference in physical assumptions between the two models is that the Eulerian model has vertical mixing explicitly modelled whereas the Lagrangian model has none. The explicit diffusion was modelled with an eddy coefficient of 50, 12.5 and 6.25 m^2 sec^{-1} for the 100, 25 and 12.5 m resolution cases, respectively.

Fig. 6 shows a comparison of the steady-state solutions for the three Eulerian cases and the one Lagrangian case for S, N and $\bar{R}$. The steady-state solutions for the Eulerian case appear to be converging to the Lagrangian parcel theory solution. *One main effect of low spatial resolution is to cause under-prediction of the droplet concentration,* i.e., the nucleation region is spread out in the vertical which causes S values to be too low, which in turn causes N to be too small, and future values of $\bar{R}$ to be too large. It is indeed encouraging that even though the 100 m resolution model does not adequately resolve the nucleation region ($\sim$50 m thick) the solution is not completely destroyed.

Some possible approaches with regard to combating the problem of low spatial resolution in a microphysical cloud model of this type come to mind. The first is to bias the initial nuclei conditions toward continental conditions in order to make up for the effects of low spatial resolution. A second approach might be to consider a mixed Eulerian-Lagrangian model. This appears to be a challenging and possibly important problem in the field of cloud modelling.

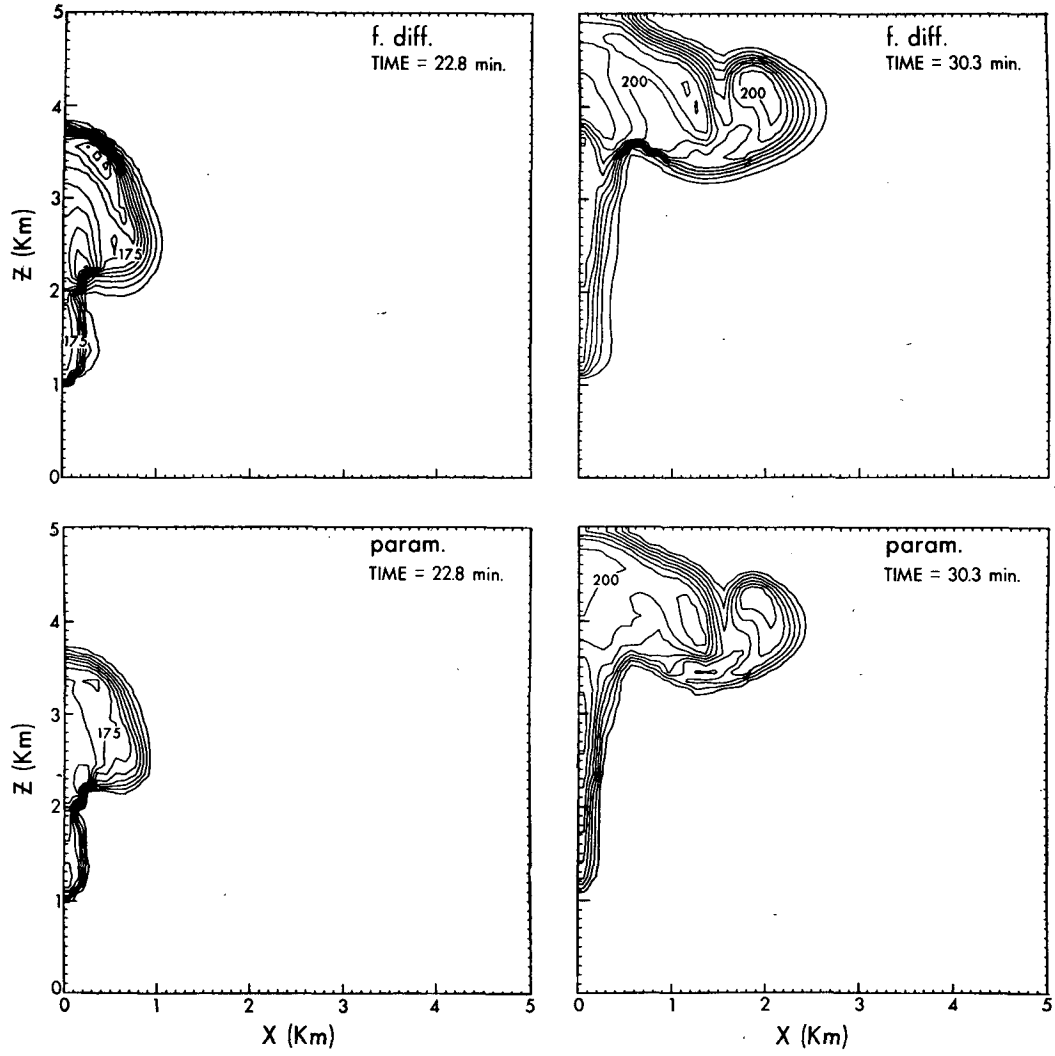

FIG. 11. As in Fig. 8 except for N fields with a contour interval of 25 cm^{-3}.

5. Application of the parameterized scheme in a fully time-dependent cloud model

Clark (1973) presented a two-dimensional microphysical cumulus model in which one example (run II) was presented where only nucleation and condensation-evaporation theories were modelled. In his model he had 37 droplet-raindrop categories with radii ranging from 0.6 to 2314 μm. Also, there were 40 nuclei categories which were used to represent the physics of nucleation. The spatial grid resolution was 100 m with 50 vertical and 150 horizontal grids. The same example will now be presented except that the finite-difference microphysics package is replaced with the parameterized microphysics described in this paper. This run used the adaption of Warner's (1969) nuclei distribution as given by (32).

The convection was initiated by a warm bubble in the 1-km neutral layer as was the case in run II. There is one small difference in the formulation of the dynamics between run II and the present case. Between the time run II was performed and the present calculations, the Clark model had been generalized to allow for nonlinear eddy coefficients (Smagorinsky, 1963) so that the diffusion terms for momentum are slightly different. In the present model the momentum equations are given by

$$\frac{\partial}{\partial t}(\rho w)=\cdots+\frac{\partial}{\partial z}(\rho KG)+\frac{\partial}{\partial x}(\rho KD), \tag{33}$$

$$\frac{\partial}{\partial t}(\rho u)=\cdots+\frac{\partial}{\partial z}(\rho KD)-\frac{\partial}{\partial x}(\rho KG), \tag{34}$$

where

$$D=\frac{\partial w}{\partial x}+\frac{\partial u}{\partial z}, \tag{35}$$

$$G=\frac{\partial w}{\partial z}-\frac{\partial u}{\partial x}. \tag{36}$$

The present formulation is taken from Lilly (1962) and reduces to exactly the same form as used by Clark when the velocity divergence is set equal to zero in these models. The difference in the momentum diffusion formulation appears to have caused some slight differences in the resulting flow. The maximum values of the streamfunction at the latter times of the models integration were slightly larger for run II than for the present case. The differences were so slight that the author did not consider it worthwhile to change the model's formulation back to its previous form in order to run this comparison experiment.

Fig. 7 shows a comparison between the maximum vertical velocity for runs I and II of Clark (1973) and the present case. Run I was an experiment where no microphysics had been included, i.e., R.H. = 100% during condensation, with instantaneous evaporation if R.H. < 100%. The present case and run II are almost identical whereas the deviations between runs I and II are much larger.

Figs. 8, 9, 10 and 11 display field comparisons between run II and the present case for the C_d, $\bar{R}$, S and N fields. Two time levels are shown, the latest time of which ($t=30.3$ min) represents the time level at which run II was terminated. The parameterized C_d fields fall approximately halfway between runs I and II (only run II C_d is shown) in regions of evaporation. One possible reason for this is that the parameterized evaporation calculations did not consider accomodation coefficient effects which result in larger evaporation rates for the parameterized model. Also, differences in implicit diffusion of q_c in the evaporation regions may account for the differences in C_d between the microphysical and parameterized model.

The $\bar{R}$ fields (Fig. 9) compare very well qualitatively but there are quantitative differences. The $\bar{R}$ values are slightly higher for the parameterized model, most likely because the parameterized model predicted higher N values. Since q_c values were very similar, positive differences in N result in negative differences in $\bar{R}$. Another contributing factor to the difference between $\bar{R}$ plots is that the spectra widths in run II were typically larger than in the present case. In run II, μ was always larger than 0.2 whereas in the present case μ attained minimum values of 0.05 (which was the arbitrary lower limit imposed). The large values of μ predicted by run II, although reasonably realistic, were most likely influenced by truncation error. Unfortunately, this is one parameter which the conventional microphysical models do not seem to be able to even qualitatively predict due to their rather low spatial resolution. At any rate, a narrower spectrum results in a slightly larger value of $\bar{R}$ for a given q_c.

The S field comparisons in Fig. 10 clearly show the tendency for the parameterized model to have lower values of S resulting in a more maritime cloud character, since the same aerosol distribution was assumed for both runs. The neglect of accomodation coefficient effects in the parameterized model was probably the main reason for the differences in maximum S values during nucleation. At the time of these numerical experiments the author did not know of a simple method of including such effects using only a single gamma distribution. Recently, it has been found possible to include such effects (using a single gamma distribution) and this method will be described in the future. The parameterized model can be seen to have had the effect of confining the nucleation region to one grid point. As will be seen in a later figure, the S_{max} oscillations still persist.

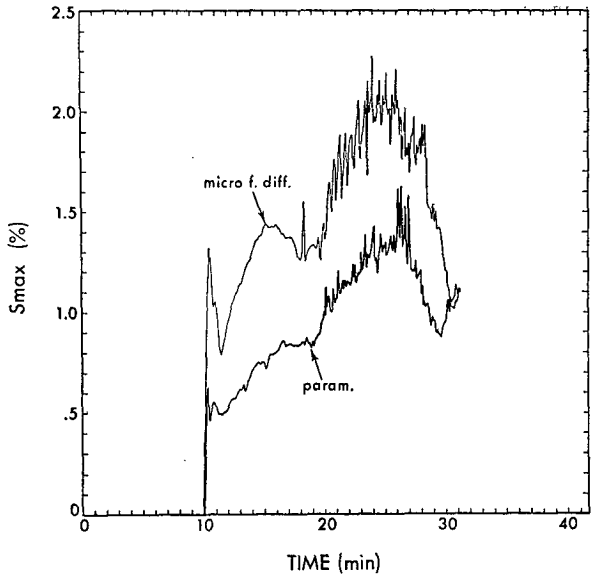

FIG. 12. S_{max} vs t for run II of Clark (1973) and the present two-dimensional parameterized solution.

The N fields (Fig. 11) also compare relatively well except that as before the parameterized model is more maritime in character.

Fig. 12 shows S_{max} vs t for run II and the present case. The parameterized model has lower S_{max} values by $\sim$0.5%. The oscillations still persist in the present case and are attributed to low spatial resolution. These oscillations occur in the nucleation regions of the modelled clouds.

Thus, a comparison of the two-dimensional cloud model results suggest that most of the differences may be due to the fact that accommodation coefficient effects were considered in Clark (1973) but were neglected in the present parameterized model. This is probably why the present fields are more maritime in character than run II of Clark (1973).

6. Conclusions

The parameterization of the cloud phase was successfully applied to three cloud model calculations. The scheme was tested in a Lagrangian bubble calculation, a one-dimensional Eulerian calculation, and a two-

dimensional Eulerian calculation. In each of the above cases, the parameterized solution was compared with an equivalent finite-difference type microphysical calculation where a specified number of radius categories was used to describe the droplet spectra.

The Lagrangian bubble application of the parameterization gave very accurate results for S, N, $\bar{R}$ and μ. In the one-dimensional Eulerian calculation, it was shown that the effect of poor spatial resolution (for the parameterized model) in regions of nucleation is to make the microphysical solutions more maritime in character, i.e., lower N values with lower spatial resolution.

The two-dimensional Eulerian finite-difference calculations of Clark (1973) were rerun using the parameterized model. Qualitatively, as well as quantitatively, the solutions of N, $\bar{R}$ and S compare very accurately. One difference between the two solutions was that the nucleation region spread out with higher $S_{\max}$ values for the finite-difference approach. Treatment of a single distribution function (gamma) for the cloud droplets resulted in sharper gradients of N and $\bar{R}$ for the parameterized model. This had the effect of confining the nucleation region to a single grid point in the vertical. This is considered an advantage of the gamma distribution approach because the vertical dimensions of the nucleation region are likely to be smaller than a single grid point (100 m).

The results of this paper are encouraging to the continued microphysical modelling of clouds because it has been shown that poor resolution of nucleation regions appears to have only a slight quantitative effect on the prediction of the microphysical variables. For example, the difference between N predictions using 100 m vertical grids was only 15% lower than the 12.5 m vertical grid case for a one-dimensional calculation presented.

APPENDIX

Truncation Errors in Microphysical Eulerian Cloud Models Associated with Condensation Theory

Microphysical cloud models which treat the dynamics as well as the microphysics of condensation in Eulerian formulation will be affected by truncation errors in the time, radius and spatial dimensions. A simple example will be considered in order to estimate the radius and spatial resolutions required to accurately represent the analytical equations in second-order finite difference formulation.

The steady-state equation

$$w\frac{\partial f}{\partial z}+\frac{\partial}{\partial r}\left(\frac{dr}{dt}f\right)=0 \tag{A1}$$

describes a balance between advection and diffusional growth for the droplet density function f. This type of steady-state assumption for f might be a reasonable approximation for a cloud edge evaporation region or for a cloud base region where we are considering sizes of droplets considerably larger than the radii of any freshly activated nuclei. The vertical air velocity w will be assumed constant and the diffusional growth rate dr/dt of a droplet of radius r will be taken as

$$\frac{dr}{dt}=\frac{kS}{\bar{R}}=V_{\bar{R}}=\text{constant}, \tag{A2}$$

where $\bar{R}$ is the mean radius, S the percent supersaturation and $k\approx 1$ $(\mu\text{m})^2$ sec^{-1}. Eq. (A1) now reduces to the linear form

$$w\frac{\partial f}{\partial z}+V_{\bar{R}}\frac{\partial f}{\partial r}=0. \tag{A3}$$

The second-order finite-difference approximation of (A3) is taken as

$$(w/2\Delta z)[f(r,z+\Delta z)-f(r,z-\Delta z)] +(V_R/2\Delta r)[f(r+\Delta r,z)-f(r-\Delta r,z)]=0, \tag{A4}$$

where Δz and Δr are the grid increments in the spatial and radius dimensions, respectively. Expanding terms in a Taylor's series we have

$$[f(r,z+\Delta z)-f(r,z-\Delta z]/(2\Delta z) =\frac{\partial f}{\partial z}+\frac{\Delta z^2}{6}\frac{\partial^3 f}{\partial z^3}+\text{O}(\Delta z^4), \tag{A5}$$

$$[f(r+\Delta r,z)-f(r-\Delta r,z)]/(2\Delta r) =\frac{\partial f}{\partial r}+\frac{\Delta r^2}{6}\frac{\partial^3 f}{\partial r^3}+\text{O}(\Delta r^4). \tag{A6}$$

In order for (A4) to be an accurate approximation of (A3), we require

$$\left|\frac{\Delta z^2}{6}\frac{\partial^3 f}{\partial z^3}\right|\ll\left|\frac{\partial f}{\partial z}\right|, \tag{A7}$$

$$\left|\frac{\Delta r^2}{6}\frac{\partial^3 f}{\partial r^3}\right|\ll\left|\frac{\partial f}{\partial r}\right|. \tag{A8}$$

Also, a practical requirement is that

$$\left|w\Delta z^2\frac{\partial^3 f}{\partial z^3}\right|\sim\left|V_{\bar{R}}\Delta r^2\frac{\partial^3 f}{\partial r^3}\right|, \tag{A9}$$

so that we have similar accuracy in both dimensions.

The density function will be assumed to take the form

$$f=N(\sqrt{2\pi}\sigma)^{-1}\exp[-(r-\bar{R})^2/2\sigma^2], \tag{A10}$$

where σ^2 is the variance, N the total number of particles between $r=0$ to $+\infty$ (it is being assumed then that $\bar{R}\gg\sigma$), $\bar{R}$ the mean radius, and $\sigma/\bar{R}$ the coefficient of

dispersion μ. From (A2) and (A3) we have

$$\frac{\partial \bar{R}}{\partial z}=\frac{V_{\bar{R}}}{w}, \tag{A11}$$

which with (A10) will allow an estimation of the magnitudes of the various derivatives in (A7)–(A9).

The assumption is now made that, in order to predict μ, (A4) should be accurate at $r=\bar{R}\pm\sigma$. This reduces (A7)–(A9) to

$$(\Delta r/\bar{R})^2 \ll 3\mu^2, \tag{A12}$$

$$\Delta z \sim \Delta r \bar{R} w/(kS), \tag{A13}$$

where (A10) and (A11) have been applied. Eqs. (A12) and (A13) can be used to estimate the radius resolution required to accurately represent diffusion growth at $r=\bar{R}\pm\sigma$ and the spatial resolution required to maintain the same degree of accuracy, respectively. For the simplified case, it is apparent from (A12) and (A13) that the accuracy of the solutions to (A3) depend on both spatial and radius domain resolution. *This point should be considered by modellers when they are increasing the number of spectral categories in their cloud model in order to better represent the evolution of the droplet spectrum.*

Of course, no account was taken in this Appendix of how large (or small) μ should actually be as a result of the prediction equations. If microphysical modellers use the "proper" equations which actually simulate nature, then μ should be equal to observed values. At the same time, there is still likely to be a strong balance between advection and diffusional growth so that (A12) and (A13) can be used to determine whether truncation error had a strong effect on determining μ or whether it was actually determined by the specified equations, initial conditions and boundary conditions imposed.

Consider the resolution which might be required at about 50–100 m above cloud base: $\bar{R}=5$ μm and $\mu=0.2$ would require [from (A12)] $\Delta r \ll 1.7$ μm. Say we let $\Delta r=0.3$ μm, then with $S=0.5\%$ and $w=2$ m sec^{-1}, we would require [from (A13)] $\Delta z=6$ m. Even the presently published one-dimensional models are far from having this high a resolution. Evaporation region calculations could require even higher spatial resolution because the absolute value of S could be much larger.

Acknowledgments. The author wishes to thank Drs. K. Miyakoda, J. Mahlman, F. Lipps and B. Hoskins for their helpful discussions and criticism of the manuscript. The author is indebted to Dr. J. Smagorinsky as well as many other GFDL members for their support. This work was sponsored by the National Research Council of Canada through a post-doctoral fellowship and by the Geophysical Fluid Dynamics Laboratory, NOAA, under Grant E22-21-70(G).

REFERENCES

Árnason, G., and R. S. Greenfield, 1972: Micro- and macrostructures of numerically simulated convective clouds. *J. Atmos. Sci.*, **29**, 342–367.

Berry, E. X, 1965: Cloud droplet growth by collection. Ph.D. dissertation, University of Nevada, Reno.

Clark, T. L., 1973: Numerical modelling of the dynamics and micro-physics of warm cumulus convection. *J. Atmos. Sci.*, **30**, 857–878.

Cotton, W. R., 1972: Numerical simulation of precipitation development in supercooled cumuli. Part I. *Mon. Wea. Rev.*, **100**, 757–763.

Crowley, W. P., 1968: Numerical advection experiments. *Mon. Wea. Rev.*, **96**, 1–11.

Fletcher, N. H., 1962: *The Physics of Rainclouds*. Cambridge University Press, 390 pp.

Kessler, E., 1967: On the continuity of water substance. ESSA Tech. Memo. IERTM–NSSL 33.

Levin, L. M., 1958: Functions to represent drop size distributions in clouds. The optical density of clouds. *Izv. Akad. Nauk SSSR, Ser. Geofiz.*, **10**, 698–702.

Lilly, D. K., 1962: On the numerical simulation of buoyant convection. *Tellus*, **14**, 148–172.

Smagorinsky, J., 1963: General circulation experiments with the primitive equations: 1. The basic experiment. *Mon. Wea. Rev.*, **91**, 99–164.

Twomey, S., 1959: The nuclei of natural cloud formation. Part II: The supersaturation in natural clouds and the variation of cloud droplet concentration. *Geofis. Pura Appl.*, **43**, 243–249.

Warner, J., 1969: The microstructure of cumulus cloud. Part II: The effect on droplet size distribution of the cloud nucleus spectrum and updraft velocity. *J. Atmos. Sci.*, **26**, 1272–1282.